Iterative Receiver for Power-Domain NOMA with Mixed Waveforms

Martin Sigmund *, Roberto Bomfin *, Marwa Chafii†‡, Ahmad Nimr *, Gerhard Fettweis *
*Vodafone Chair Mobile Communication Systems, Technische Universität Dresden, Dresden, Germany
{martin.sigmund,roberto.bomfin,ahmad.nimr,gerhard.fettweis}@tu-dresden.de
† Engineering Division, New York University (NYU) Abu Dhabi, Abu Dhabi, UAE
‡ NYU WIRELESS, NYU Tandon School of Engineering, New York, USA
marwa.chafii@nyu.edu

***Abstract*—Power-domain non-orthogonal multiple access (NOMA) is a promising radio access technique with non-orthogonal resource allocation that provides a greater spectrum efficiency than the conventional orthogonal multiple access (OMA). In this paper, an iterative receiver is derived for NOMA. It is based on soft-information successive interference cancellation (SIC) combined with a minimum mean square error parallel interference cancellation (MMSE-PIC) detector. Orthogonal frequency division multiplexing (OFDM) is usually the typical waveform employed. However, with the proposed receiver design, any linear modulation can be used. In addition to OFDM, single-carrier (SC) and the recently proposed sparse Walsh-Hadamard (SWH) are investigated. The NOMA scheme is analysed in a multi-path fading channel, where two users have different power ratios and waveforms. Simulation results show that mixing OFDM and SWH for a two-user NOMA gives the best performance with low receiver complexity.**

***Index Terms*—power-domain non-orthogonal multiple access (NOMA), waveforms, successive interference cancellation (SIC), iterative receiver**

I. Introduction

Serving multiple users simultaneously is of major importance in modern communication systems. In the previous cellular systems, orthogonal multiple access (OMA) is considered to enable an easy separation of the signals at the receiver. A variety of orthogonal waveforms have been used, each with their advantages and disadvantages. The orthogonality can be achieved in multiple domains based on time, frequency, code, or space division multiplexing. However, the use of orthogonal signals is not optimal in terms of the achievable multiuser data rate [1]. With the increase of demands on communication services, it is required to develop alternative access schemes for a more efficient utilization of the available resources, in particular the frequency resources in the sub-6 GHz frequency bands. Accordingly, non-orthogonal multiple access (NOMA) has been proposed to increase the capacity of cellular networks through the reuse of the time-frequency-code resources for multiple users. With NOMA, a lower outage probability can be achieved and the achievable data rate can be increased compared to the widely deployed orthogonal frequency division multiple access (OFDMA) [2], [3].

The NOMA schemes can be divided into two main categories: code-domain NOMA and power-domain NOMA. In code-domain NOMA, sparse or non-orthogonal cross correlation sequences of low correlation coefficient are utilized for the user-specific spreading sequences [2]. In power-domain NOMA, the signals of the different users are superimposed on each other. For the downlink, the signals are superimposed at the transmitter and in the uplink, the superposition occurs through the wireless channel. Therefore, multiple users can utilize the same time-frequency resource and their respective signals needs to be decoupled at the receiver using multi user detection (MUD) algorithms like successive interference cancellation (SIC) [1]. The drawbacks of using NOMA are the increased complexity of the system, especially the receiver, and the performance degradation because of the SIC and channel estimation errors [4].

Typically, NOMA is implemented for multiple users using the same waveform, e.g. orthogonal frequency division multiplexing (OFDM), leading to a simple implementation. Recently, several publications have proposed the superposition of different waveforms. The partial overlap of OFDMA and single-carrier frequency division multiple access (SC-FDMA) is analysed in [5], where an adaptive MUD scheme based on iterative likelihood testing and signal-to-interference-plus-noise ratio (SINR) processing is derived. This MUD approach outperforms the conventional SIC. However, the considered channel is flat Rayleigh fading, which leads to an insignificant gain in terms of the bit error rate (BER) performance when combining different waveforms. In [6], an iterative receiver for NOMA with OFDM and multicarrier (MC) code-division multiple access (CDMA) is derived, showing the advantages of soft-decision over hard-decision receivers. Although it is a NOMA system, the receiver still works without a power imbalance. Considering heterogeneous mobility of the users, a transmission protocol exploiting NOMA is proposed in [7]. The users are grouped in different mobility profiles. The data of the high mobility user is transmitted with orthogonal time frequency space (OTFS), which spreads the symbols in the delay-Doppler plane, whereas OFDM is employed for low-mobility users. The constructed NOMA system spreads the signal of the high-mobility users over a large time-frequency resource for high detection reliability while ensuring sufficient bandwidth for the low-mobility ones. The mixture of OFDM and OFDM with index modulation (OFDM-IM) is proposed in [4]. This is achieved by assigning a higher power level for the active subcarriers used in OFDM-IM. By employing interference cancellation (IC) and low-density parity-check (LDPC) codes, it is shown that this scheme outperforms the conventional power-domain NOMA which utilizes OFDM for all users.

Unlike the aforementioned papers where the receiver design is specific to the employed waveforms, this work derives a framework to enable the use and combination of any linearly modulated waveforms. In addition, we design a generic iterative receiver that performs reprocessing of incorrectly detected blocks to enhance the block error rate (BLER) performance. Moreover, this paper considers a realistic frequency-selective channel (FSC) and is not limited to an additive white Gaussian noise (AWGN) channel as in [6] or a flat fading channel as in [5]. The novel receiver is based on a minimum mean square error parallel interference cancellation (MMSE-PIC) detector for OMA [8], [9]. This is extended for NOMA with the a-priori knowledge about the interference. The main contributions of this paper are: 1) Derivation of a generic iterative receiver based on soft-information SIC with a MMSE-PIC detector for uplink power-domain NOMA. 2) SIC errors are a major limitation for NOMA systems. Hence, the quality of the soft a-priori estimates generated by the iterative MMSE-PIC detector for the IC is analysed. 3) Evaluation of the NOMA system with OFDM, single-carrier (SC), sparse Walsh-Hadamard (SWH), and their combination. Mixed waveforms are proposed to exploit, first, the better quality of the a-priori estimates of the strong user with OFDM for the IC of the weak user and, second, the advantage of frequency spreading waveforms for the low signal-to-noise ratio (SNR) user.

The remainder of the paper is organized as follows: Section II introduces the system model. Section III is dedicated to the design of the generic iterative receiver. Section IV provides numerical results. Finally, Section V concludes the paper.

II. System model

A synchronized uplink NOMA system is depicted for three transmitters and one base station in Fig. 1. A major difference to the downlink is that even though the blocks are overlapping in power domain, they have been transmitted through different channels $\boldsymbol{h}_1, \boldsymbol{h}_2, \boldsymbol{h}_3$. The superimposed received signal in the time domain is given as

$$\tilde{y}[n] = \sum_{k=1}^{K} \sqrt{P_k} h_k[n] * x_k[n] + w[n], \tag{1}$$

with the transmission samples $x_k[n]$ of the kth user, the channel impulse response $h_k[n]$ and the AWGN $w[n]$. The symbol $*$ describes the linear convolution. Instead of amplifying the transmission sequence with the transmission power, we combine, for simplicity, the transmission power with the channel gain which yields to the received power P_k and the received power ratio $10\log_{10}(P_k/P_n)$ between the received power caused by the kth and nth user. It is assumed that the channel state information (CSI) is available at the receiver. The transmission system is visualized in Fig. 2.

A. Wireless Channel

In this work, an FSC is assumed whose impulse response for the kth user is given as $\boldsymbol{h}_k = [h_{k,0}, h_{k,1}, \ldots, h_{k,L-1}]$. $h_{k,l}$ is a stationary complex Gaussian process [10, p. 128] which is uncorrelated with respect to (w.r.t.) k and l, for $k \in \{1, 2, \ldots, K\}$ and $l \in \{0, 1, \ldots, L-1\}$, respectively. The baseband channel is assumed to be invariant over the entire transmission time. The power delay profile (PDP) model defines the power ρ_l of an arbitrary lth path as a random process with the correlation function given by

$$\mathbb{E}\{h_{k,l} h^{\mathrm{H}}_{k',l'}\} = \rho_l \delta[k-k'] \delta[l-l'], \tag{2}$$

with the discrete Dirac pulse $\delta[n]$. If the length of the cyclic prefix (CP) is longer than the channel delay spread, the channel can be modelled as a circular convolution which can be described easily in the frequency domain. The circulant channel matrix based on $\boldsymbol{h}_k$ is called $\boldsymbol{H}_k$. For an easy description of the received signal in the frequency domain, the diagonal matrix $\boldsymbol{\Lambda}_k = \boldsymbol{F}\boldsymbol{H}_k\boldsymbol{F}^{\mathrm{H}}$ is used, whose elements correspond to the channel response of the kth user in the frequency domain.

B. Linear Modulation Model

1) Transmitter: For each user k, a number of bits are generated. These bits are assumed to be uniformly distributed random bits $\boldsymbol{b}_k \in \{0,1\}^{N_b}$. Precoding leads to the coded bits $\boldsymbol{c}_k \in \{0,1\}^{N_c}$. The number of coded bits N_c is dependent on the number of the uncoded bits N_b and the code rate r. The coded bits are mapped to a quadrature amplitude modulation (QAM) constellation set $\mathcal{S}$ with the cardinality $|\mathcal{S}| = J$. This results in the symbol vector $\boldsymbol{d}_k \in \mathcal{S}^{N_d}$ such that $\mathbb{E}\{\boldsymbol{d}_k \boldsymbol{d}_k^{\mathrm{H}}\} = \mathbf{I}_{N_d}$ holds. The operators $\mathbb{E}[\cdot]$, $(\cdot)^{\mathrm{H}}$ and the symbol $\mathbf{I}$ denote respectively the statistical expectation, the Hermitian transpose and the identity matrix. The number of symbols is $N_d = N_c/\log_2(J)$. The symbols are multiplied with the modulation matrix in the time domain $\boldsymbol{A}_{\mathrm{T}_k} \in \mathbb{C}^{N_d \times N_d}$ of the kth user. The transmission samples are expressed as $\boldsymbol{x}_k = \boldsymbol{A}_{\mathrm{T}_k}\boldsymbol{d}_k$ in the time domain and $\boldsymbol{X}_k = \boldsymbol{A}_{\mathrm{F}_k}\boldsymbol{d}_k$ in the frequency domain, where the transmission frequency-domain matrix is given by $\boldsymbol{A}_{\mathrm{F}_k} = \boldsymbol{F}\boldsymbol{A}_{\mathrm{T}_k}$. Here, $\boldsymbol{F}$ refers to the normalized discrete Fourier transform (DFT) matrix. To enable a simple frequency-domain equalization, a CP with the length N_{CP} is appended to $\boldsymbol{x}_k$ resulting in a block. Hereafter, a CP insertion is assumed for all waveforms. Next, the waveforms used in this work are introduced.

2) Waveforms: If the CSI is only available at the receiver and the transmitted symbols are independent, a unitary linear modulation matrix has no impact on the capacity. However, in a real transmission system, the input signal is not Gaussian distributed as in the capacity analysis. Due to the use of a discrete constellation set and the information rate limit, the mutual information is influenced by the transmitter matrix [11]. Under the assumption of perfect feedback equalization, it is shown that an optimal waveform needs to spread the data over the domain of selectivity of the channel [11].

In this paper, we focus on an FSC such that an optimal transmission matrix spreads the symbols over the bandwidth leading to the same channel gain for all symbols. Among the waveforms that fulfill this criterion are SC-FDMA (referred as SC) and SWH precoded OFDM (referred as SWH). In the time domain, OFDM spreads its symbols fully, SWH partly while SC does not employ any spreading. In the frequency domain, SC spreads fully, SWH partly while OFDM does not employ spreading.

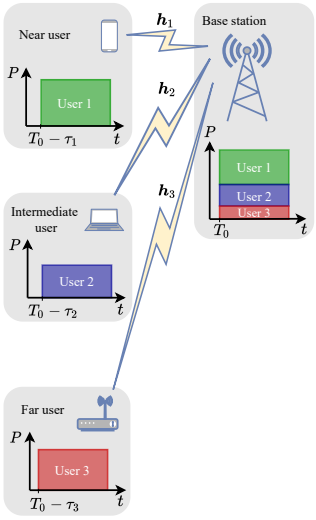

Fig. 1: Uplink NOMA scenario with three-user equipment and one base station.

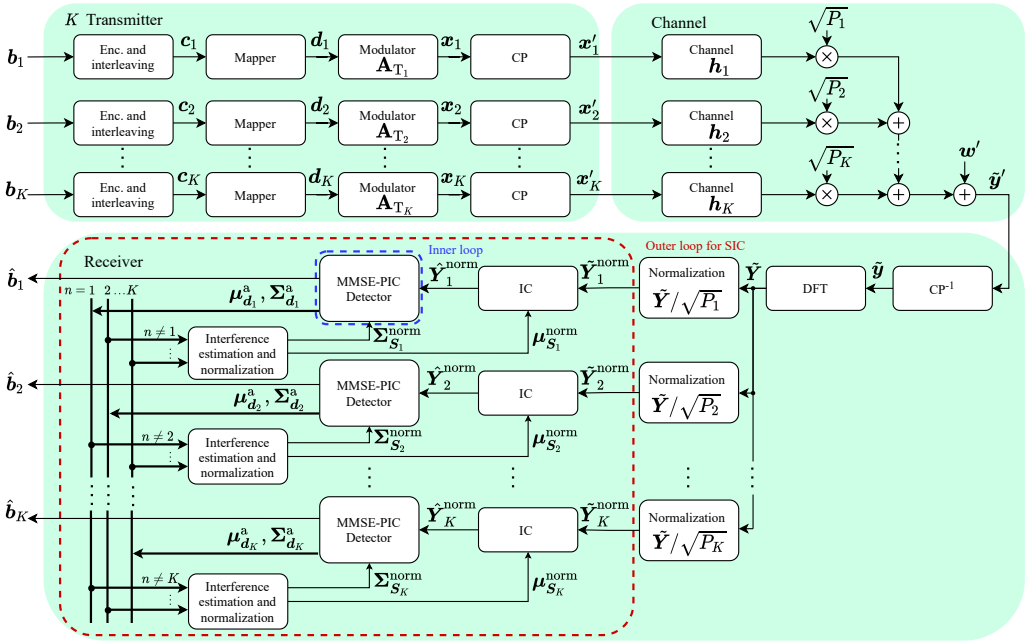

Fig. 2: System overview.

For the reference waveforms OFDM and SC, the transmission matrices are $\boldsymbol{A}_{\mathrm{T}}^{\mathrm{OFDM}} = \boldsymbol{F}^{\mathrm{H}}$ and $\boldsymbol{A}_{\mathrm{T}}^{\mathrm{SC}} = \mathbf{I}$, respectively. In [12] the SWH precoded OFDM is presented. It has been proven that the equal gain condition can be satisfied for frequency-domain sparsity if the spreading factor $Q \geq L$ with L being the channel delay spread. Therefore, a similar performance as SC can be achieved, but with a significantly reduced complexity. The transmission matrix is $\boldsymbol{A}_{\mathrm{T}}^{\mathrm{SWH}} = \boldsymbol{F}^{\mathrm{H}}\boldsymbol{U}$. The precoding matrix $\boldsymbol{U} \in \mathbb{R}^{N_d \times N_d}$ can be computed as [12] $\boldsymbol{U} = \boldsymbol{V}_Q \otimes \mathbf{I}_Z$. The Kronecker product is denoted as $\otimes$. It applies $N_d = QZ$, and the Walsh-Hadamard (WH) matrix is computed recursively as

$$\boldsymbol{V}_m = \boldsymbol{V}_2 \otimes \boldsymbol{V}_{\frac{m}{2}} \text{ with } m = 2^{m'}, \{m' \in \mathbb{N}^+ : m' \geq 2\}, \quad (3)$$

$$\text{with} \quad \boldsymbol{V}_2 = \frac{1}{\sqrt{2}} \begin{bmatrix} 1 & 1 \\ 1 & -1 \end{bmatrix}. \quad (4)$$

The index of the kth user is noted as $\boldsymbol{A}_{\mathrm{T}_k}$ in the equations throughout this paper since the users can utilize different transmission matrices as $\boldsymbol{A}_{\mathrm{T}}^{\mathrm{OFDM}}$, $\boldsymbol{A}_{\mathrm{T}}^{\mathrm{SC}}$ or $\boldsymbol{A}_{\mathrm{T}}^{\mathrm{SWH}}$.

3) Received Signal: For NOMA, the received signal in the frequency domain, which is normalized to the received power of the kth user, is given as

$$\tilde{\boldsymbol{Y}}_k^{\mathrm{norm}} = \frac{\tilde{\boldsymbol{Y}}}{\sqrt{P_k}} = \boldsymbol{\Lambda}_k \boldsymbol{A}_{\mathrm{F}_k} \boldsymbol{d}_k + \boldsymbol{S}_k^{\mathrm{norm}} + \boldsymbol{W}_k^{\mathrm{norm}}, \quad (5)$$

with the normalized interference

$$\boldsymbol{S}_k^{\mathrm{norm}} = \frac{\boldsymbol{S}_k}{\sqrt{P_k}} \quad \text{with } \boldsymbol{S}_k = \sum_{n=1, n\neq k}^{K} \sqrt{P_n} \boldsymbol{\Lambda}_n \boldsymbol{A}_{\mathrm{F}_n} \boldsymbol{d}_n. \quad (6)$$

$\boldsymbol{W}_k^{\mathrm{norm}} = \boldsymbol{W}/\sqrt{P_k}$ is the frequency-domain noise which is normalized to the power of the kth user with $\sigma_k^2 = \sigma^2/P_k$. $\boldsymbol{W} \sim \mathcal{CN}(0, \sigma^2 \mathbf{I})$ is the AWGN in the frequency domain.

III. Generic Iterative Receiver Design for NOMA

The receiver needs to consider the noise and the interference of other users to reliably estimate the transmitted data. In a power-domain NOMA system, a MUD scheme should be used to detect the signals of the non-orthogonal users. Typically a SIC algorithm is utilized. The SIC appears in the decoding schedule defining in which order the blocks are computed. It is assumed that the average received power decreases from the 1st user to the Kth user as $\bar{P}_1 > \cdots > \bar{P}_K$. Therefore, the blocks are decoded from the 1st user down to the Kth user. For the respective user, the interference is estimated and cancelled, and the MMSE-PIC detector (*inner loop*) is executed. The blocks of all K users have to be processed once for each SIC iteration. To improve the estimates, the blocks can be reprocessed N_{SIC} times. All computational steps for one SIC iteration are defined as the *outer loop* as shown in Fig. 2.

A. Interference Estimation and Cancellation

The *Interference estimation and normalization* block estimates the following interference statistics. The a-priori mean of the interference of the kth user can be calculated as

$$\boldsymbol{\mu}_{\boldsymbol{S}_k}^{\mathrm{a}} = \mathbb{E}\{\boldsymbol{S}_k\} = \sum_{n=1, n\neq k}^{K} \sqrt{P_n} \boldsymbol{\Lambda}_n \boldsymbol{A}_{\mathrm{F}_n} \boldsymbol{\mu}_{\boldsymbol{d}_n}^{\mathrm{a}}, \quad (7)$$

and the a-priori covariance of the interference as follows

$$\begin{aligned} \boldsymbol{\Sigma}_{\boldsymbol{S}_k}^{\mathrm{a}} &= \mathbb{E}\{(\boldsymbol{S}_k - \boldsymbol{\mu}_{\boldsymbol{S}_k}^{\mathrm{a}})(\boldsymbol{S}_k - \boldsymbol{\mu}_{\boldsymbol{S}_k}^{\mathrm{a}})^{\mathrm{H}}\} \quad (8) \\ &= \sum_{n=1, n\neq k}^{K} P_n \mathbb{E}\{\boldsymbol{\Lambda}_n \boldsymbol{A}_{\mathrm{F}_n} (\boldsymbol{d}_n - \boldsymbol{\mu}_{\boldsymbol{d}_n}^{\mathrm{a}})(\boldsymbol{\Lambda}_n \boldsymbol{A}_{\mathrm{F}_n} (\boldsymbol{d}_n - \boldsymbol{\mu}_{\boldsymbol{d}_n}^{\mathrm{a}}))^{\mathrm{H}}\} \\ &= \sum_{n=1, n\neq k}^{K} P_n \boldsymbol{\Lambda}_n \boldsymbol{A}_{\mathrm{F}_n} \boldsymbol{\Sigma}_{\boldsymbol{d}_n}^{\mathrm{a}} \boldsymbol{A}_{\mathrm{F}_n}^{\mathrm{H}} \boldsymbol{\Lambda}_n^{\mathrm{H}}, \end{aligned}$$

where $\boldsymbol{\Sigma}^{\mathrm{a}}_{\boldsymbol{d}_n} = \mathbb{E}\{(\boldsymbol{d}_n - \boldsymbol{\mu}^{\mathrm{a}}_{\boldsymbol{d}_n})(\boldsymbol{d}_n - \boldsymbol{\mu}^{\mathrm{a}}_{\boldsymbol{d}_n})^{\mathrm{H}}\}$. To simplify the equalizer notation, the a-priori interference mean and covariance are normalized to the kth transmission power P_k as $\boldsymbol{\mu}^{\mathrm{norm}}_{\boldsymbol{S}_k} = \boldsymbol{\mu}^{\mathrm{a}}_{\boldsymbol{S}_k}/\sqrt{P_k}$ and $\boldsymbol{\Sigma}^{\mathrm{norm}}_{\boldsymbol{S}_k} = \boldsymbol{\Sigma}^{\mathrm{a}}_{\boldsymbol{S}_k}/P_k$, respectively. The a-priori mean $\boldsymbol{\mu}^{\mathrm{a}}_{\boldsymbol{d}_n}$ as well as the a-priori covariance matrix $\boldsymbol{\Sigma}^{\mathrm{a}}_{\boldsymbol{d}_n}$ are generated by the *A-priori Statistics* block (cf. Section III-B4) of the MMSE-PIC detector. It is assumed that the received blocks of the different users are uncorrelated. Therefore, the cross terms for different users in (8) are zero and the separate covariances of the interfering users can simply be summarized. The MMSE-PIC detector generates in every iteration a-priori estimates $\boldsymbol{\mu}^{\mathrm{a}}_{\boldsymbol{d}_n}$ of the symbol vector of the nth user (cf. Section III-B4). The iteration of the detector from which the a-priori estimates are used for the IC is defined as N_{IC}. If the interfering block n has not been computed, the a-priori mean is assumed to be zero $\boldsymbol{\mu}^{\mathrm{a}}_{\boldsymbol{d}_n} = \mathbf{0}$, and consequently, it has no contribution to the SIC. In the case that an interfering block is decoded correctly, which is identified by the cyclic redundancy check (CRC), the a-priori estimates are set to that correctly detected block, i.e., $\boldsymbol{\mu}^{\mathrm{a}}_{\boldsymbol{d}_n} = \boldsymbol{d}_n$, and hence, its interference can be perfectly removed. The *IC* block subtracts the estimated interference from the received signal as

$$\hat{\boldsymbol{Y}}^{\mathrm{norm}}_k = \tilde{\boldsymbol{Y}}^{\mathrm{norm}}_k - \boldsymbol{\mu}^{\mathrm{norm}}_{\boldsymbol{S}_k}. \tag{9}$$

Note that $\hat{\boldsymbol{Y}}^{\mathrm{norm}}_k$ is an estimate of the interference-free block $\boldsymbol{Y}^{\mathrm{norm}}_k$ under the assumption of perfect IC.

B. MMSE-PIC Detector

The MMSE-PIC detector is based on the implementation in [8] and [9]. Due to its use in a NOMA system, the different components of the MMSE-PIC detector are adapted and the inputs and outputs are extended as illustrated in Fig. 3. This figure represents the *MMSE-PIC* block introduced in the system overview in Fig. 2 and is referred to as *inner loop*. The *inner loop* takes as input the normalized interference cancelled signal in the frequency domain $\hat{\boldsymbol{Y}}^{\mathrm{norm}}_k$. Moreover, unlike in [9], we introduce the a-priori interference covariance matrix $\boldsymbol{\Sigma}^{\mathrm{norm}}_{\boldsymbol{S}_k}$. The outputs are the a-priori mean of the symbols of the kth user $\boldsymbol{\mu}^{\mathrm{a}}_{\boldsymbol{d}_k}$, its variance $\boldsymbol{\Sigma}^{\mathrm{a}}_{\boldsymbol{d}_k}$ and the estimated bits $\hat{\boldsymbol{b}}_k$.

1) Equalizer: The component-wise conditionally unbiased (CWCU) linear minimum mean square error (LMMSE) equalization for an OMA system is given as [9, eq. (5)]. For NOMA cases, the kth user is indexed and the interference of the other users $\boldsymbol{S}_k$ is considered. With that information and the reliability of the interference as the normalized a-priori covariance estimate of the interference $\boldsymbol{\Sigma}^{\mathrm{norm}}_{\boldsymbol{S}_k}$, the CWCU LMMSE equalizer can be formulated for the NOMA system. The a-posteriori mean is given by

$$\boldsymbol{\mu}^{\mathrm{p}}_{d_k} = \boldsymbol{\mu}^{\mathrm{a}}_{d_k} + \bar{\boldsymbol{\Gamma}}^{-1}_k \boldsymbol{A}^{\mathrm{H}}_{\mathrm{F}_k} \boldsymbol{\Lambda}^{\mathrm{H}}_k \boldsymbol{\Sigma}^{\mathrm{norm}}_{\boldsymbol{Y}_k} (\hat{\boldsymbol{Y}}^{\mathrm{norm}}_k - \boldsymbol{\Lambda}_k \boldsymbol{A}_{\mathrm{F}_k} \boldsymbol{\mu}^{\mathrm{a}}_{d_k}) \tag{10}$$

with the a-posteriori error matrix

$$\boldsymbol{\Sigma}^{\mathrm{p}}_{\boldsymbol{d}_k} = \bar{\boldsymbol{\Gamma}}^{-1}_k - \boldsymbol{\Sigma}^{\mathrm{a}}_{\boldsymbol{d}_k}. \tag{11}$$

The normalization of the CWCU LMMSE equalizer is archived with the multiplication of the inverse of the diagonal matrix $\bar{\boldsymbol{\Gamma}} = \mathrm{diag}\{\boldsymbol{\Gamma}_{1,1}, \boldsymbol{\Gamma}_{2,2}, \ldots, \boldsymbol{\Gamma}_{N_d,N_d}\}$. This forces the diagonal elements of the equalization matrix to be unitary,

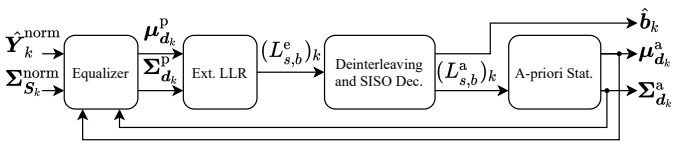

Fig. 3: *MMSE-PIC* block in NOMA (adapted from [9])

and therefore guarantees CWCU estimates of $\boldsymbol{\mu}^{\mathrm{p}}_{\boldsymbol{d}_k}$. The matrix $\boldsymbol{\Gamma}_k$ is defined as $\boldsymbol{\Gamma}_k = \boldsymbol{A}^{\mathrm{H}}_{\mathrm{F}_k} \boldsymbol{\Lambda}^{\mathrm{H}}_k \boldsymbol{\Sigma}^{\mathrm{norm}}_{\boldsymbol{Y}_k} \boldsymbol{\Lambda}_k \boldsymbol{A}_{\mathrm{F}_k}$. The covariance matrix of the signal after interference cancellation is given as

$$\boldsymbol{\Sigma}^{\mathrm{norm}}_{\boldsymbol{Y}_k} = (\boldsymbol{\Lambda}_k \boldsymbol{A}_{\mathrm{F}_k} \boldsymbol{\Sigma}^{\mathrm{a}}_{\boldsymbol{d}_k} \boldsymbol{A}^{\mathrm{H}}_{\mathrm{F}_k} \boldsymbol{\Lambda}^{\mathrm{H}}_k + \boldsymbol{\Sigma}^{\mathrm{norm}}_{\boldsymbol{S}_k} + \sigma^2_k \mathbf{I})^{-1}. \tag{12}$$

It is important to mention that due to the overall normalization to the power of the kth user, the noise variance also has to be normalized as $\sigma^2_k = \sigma^2/P_k$.

2) Extrinsic LLR: The extrinsic log-likelihood ratio (LLR) $L^{e}_{s,b}$ can be computed as in [8, eq. (15)], where b defines the bit and s the symbol. It is assumed that the noise at each constellation symbol is independent. Furthermore, the a-priori knowledge of each bit is neglected due to a marginal impact on the performance of single-input, single-output (SISO) decoders with MMSE-PIC demapping as shown in [13].

3) SISO decoder: In the SISO decoder, the a-priori LLRs of the coded bits $L^{\mathrm{a}}_{s,b}$ are calculated as in [9]. In this system, a recursive systematic convolutional code with a BCJR logarithmic maximum a posteriori (MAP) decoder is used. For simplicity, the deinterleaving of $L^{\mathrm{e}}_{s,b}$ and interleaving of $L^{\mathrm{a}}_{s,b}$ are integrated into the decoder block. The estimated information bits $\hat{\boldsymbol{b}}$ are computed by comparing the uncoded LLRs to zero. In this work, the use of a CRC is assumed. Therefore, the iterative decoding cycle stops after the correct detection, otherwise it is terminated after N_{Eq} iterations.

4) A-priori statistics of data vector: For the equalizer and the SIC, the a-priori statistics, namely, the mean $\boldsymbol{\mu}^{\mathrm{a}}_{\boldsymbol{d}}$ and the variance $\boldsymbol{\Sigma}^{\mathrm{a}}_{\boldsymbol{d}}$ are computed as in [9]. Due to unknown a-priori LLRs in the first iteration of the iterative receiver, the a-priori LLRs are assumed to be zero for all symbols, which is aligned with the assumption of equiprobability of the transmitted bits. The a-priori statistics that are used if the bits are not detected correctly, are stored after the N_{IC} iteration to be used in the interference estimation.

C. Low-complexity Considerations

The complexity of the interference covariance estimation (8) and the equalization (12) can be significantly reduced. For this it is assumed that all symbols have an equal reliability as considered in [9]. Therefore, $\boldsymbol{\Sigma}^{\mathrm{a}}_{\boldsymbol{d}_k} \approx \sigma^2_{\boldsymbol{d}_k} \mathbf{I}$ with $\sigma^2_{\boldsymbol{d}_k} = \mathrm{Tr}\{\boldsymbol{\Sigma}^{\mathrm{a}}_{\boldsymbol{d}_k}\}/N_d$. This leads to a diagonal interference covariance matrix $\boldsymbol{\Sigma}^{\mathrm{a}}_{\boldsymbol{S}_k} \approx \sum_{n=1, n\neq k}^{K} P_n \sigma^2_{\boldsymbol{d}_n} \boldsymbol{\Lambda}_n \boldsymbol{\Lambda}^{\mathrm{H}}_n$ and to $\boldsymbol{\Lambda}_k \boldsymbol{A}_{\mathrm{F}_k} \boldsymbol{\Sigma}^{\mathrm{a}}_{\boldsymbol{d}_k} \boldsymbol{A}^{\mathrm{H}}_{\mathrm{F}_k} \boldsymbol{\Lambda}^{\mathrm{H}}_k \approx \sigma^2_{\boldsymbol{d}_k} \boldsymbol{\Lambda}_k \boldsymbol{\Lambda}^{\mathrm{H}}_k$. Here, $\mathrm{Tr}\{\cdot\}$ denotes the trace of a matrix. With the approximations, (12) has a diagonal structure so that the matrix inverse can be calculated element-wise, which considerably reduces the complexity. The approximations are valid due to the use of the SC and SWH waveforms which results in a wide spread in the frequency domain. However, some information is lost as a result of

the neglected reliability of the individual symbols. To further decrease the complexity, the sparse structure of the SWH transmission matrix can be exploited as explained in [12]. Therefore, the modulation and demodulation can be computed more efficiently for SWH than for SC.

IV. Numerical Evaluation and Discussion

$K = 2$ users are considered for the NOMA simulations. The data block contains $N_d = 128$ samples and the CP has a length of $N_{\text{CP}} = 16$ samples. The length of the CP is longer than the channel delay spread, which has a length of $L = 12$ samples. Therefore, the length of the CP is sufficient. The simulated bandwidth is $B = 4.32\,\text{MHz}$. For the constellation set 4-QAM is used. The code rate is $r = 1/2$. A recursive systematic convolutional channel code with the generator polynomial $[1\ 13/15]_8$ is used for the encoder as described in [14]. For the decoding, a BCJR log-MAP algorithm is implemented. For the PDP the extended vehicular A (EVA) channel model is used [15]. The amount of SIC iterations remains variable as $N_{\text{SIC}} \in \{1, 2\}$iterations. The maximal amount of iterations of the MMSE-PIC detector is fixed to $N_{\text{Eq}} = 7$ iterations. In the case of unsuccessful detection, which is determined by the CRC check, the a-priori information is provided by the $N_{\text{IC}} = 1$ iteration of the MMSE-PIC loop for the IC stage. Note that N_{Eq} and N_{IC} are only relevant when spreading waveforms are used. The SWH spreading factor is set to $Q = 16$ with $Q \geq L$ to attain an equal gain of the symbols as proven in [12].

A. Analysis of Estimates for Interference Cancellation

To differentiate between the impact of the BLER and the quality of the a-priori estimates, represented by $\text{MSE}(\boldsymbol{\mu}^{\text{a}}_{\boldsymbol{d}_k})$ and $\text{MSE}(\boldsymbol{\Sigma}^{\text{a}}_{\boldsymbol{d}_k})$, the mean squared error (MSE) only considers a-priori estimates if the blocks are decoded incorrectly. For simplicity, the analysis of the results for both metrics are provided for the 1st user and $N_{\text{SIC}} = 1$ in Fig. 4 and 5. The trends can be recognized and transferred to the other user and multiple SIC iterations. In order to determine the impact of the MMSE-PIC iteration, N_{IC}, which is used to provide the a-priori estimates to the IC, the $\text{MSE}(\boldsymbol{\mu}^{\text{a}}_{\boldsymbol{d}_1})$ and $\text{MSE}(\boldsymbol{\Sigma}^{\text{a}}_{\boldsymbol{d}_1})$ for the 1st user for incorrectly detected blocks is shown in Fig. 4a and 4b, respectively. In both plots, the MSE of the a-priori mean estimate is significantly lower for OFDM than for SC, independently of the MMSE-PIC iteration which is used to generate the a-priori information to calculate the MSE. This shows that even though SC has a better BLER performance during the first SIC round, i.e $N_{\text{SIC}} = 1$, the soft information provided by the MMSE-PIC for the IC may not be better as well. This can be explained as follows: In the received signal of an OFDM system, both the desired signal as well as the interference are uncorrelated w.r.t. the frequency-domain samples n. There is no inter-symbol interference (ISI) and therefore no need to compute multiple MMSE-PIC iterations. For SC there is ISI and consequently multiple MMSE-PIC iterations have to be computed. In the used MMSE-PIC detector, multiple iterations lead to a convergence behaviour and in an ideal case all the ISI is removed. However, if the detection

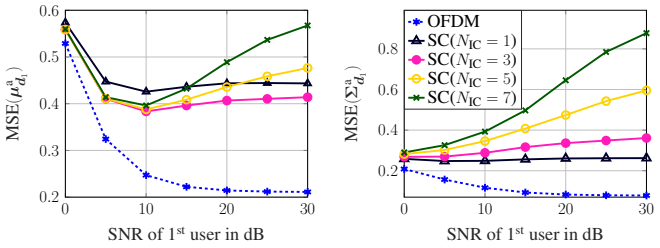

(a) Mean (b) Variance

Fig. 4: MSE of the a-priori estimates of the 1st user for incorrectly detected blocks for a power ratio of 5 dB and $N_{\text{SIC}} = 1$

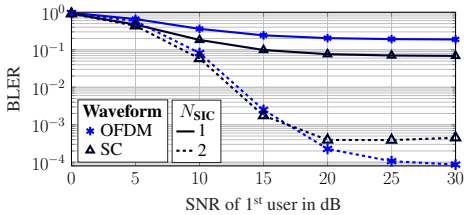

Fig. 5: BLER of the 1st user for a power ratio of 5 dB

is faulty, the receiver can converge to incorrect values. This can be seen in the quality of the variance estimate $\text{MSE}(\boldsymbol{\Sigma}^{\text{a}}_{\boldsymbol{d}_1})$ especially at high SNRs. There, the MSE increases if the a-priori information is generated at higher MMSE-PIC iterations N_{IC}. However, if the quality of the mean estimate $\text{MSE}(\boldsymbol{\mu}^{\text{a}}_{\boldsymbol{d}_1})$ is considered, the lowest MSE appears at $N_{\text{IC}} = 3$. A fraction of the ISI could be removed and the convergence behaviour is only visible for $N_{\text{IC}} > 3$. Nonetheless, the best average BLER for both users can be achieved with $N_{\text{IC}} = 1$ which is used from here on. The further processing of incorrectly detected blocks is enabled with another round of SIC, i.e. $N_{\text{SIC}} = 2$, which leads to a significantly decreased BLER for both SC and OFDM compared to $N_{\text{SIC}} = 1$ as seen in Fig. 5.

B. Comparison of Waveforms

The idea of utilizing mixed waveforms is that for the strong user any waveform achieves a low BLER, but OFDM is preferred due to its better a-priori estimates for the IC. However, for the weak user, frequency spreading leads to a significant performance gain suggesting the use of SC or SWH. The BLER curves of the 1st and the 2nd user for $N_{\text{SIC}} = 2$ are shown in Fig. 6a and 6b, respectively. The combination of waveforms is described as (waveform 1st user, waveform 2nd user).

At the high power ratio of 15 dB, the best performance for the 1st user is achieved using (SC,SC) and (SWH,SWH) which spread their symbols in the frequency domain. The other waveform combinations have a similar BLER but worse by 3 dB compared to (SC,SC). However, the system performance is dominated by the BLER of the weaker signal of the 2nd user, where all waveform combinations have a similar performance except (OFDM,OFDM) which has a higher BLER.

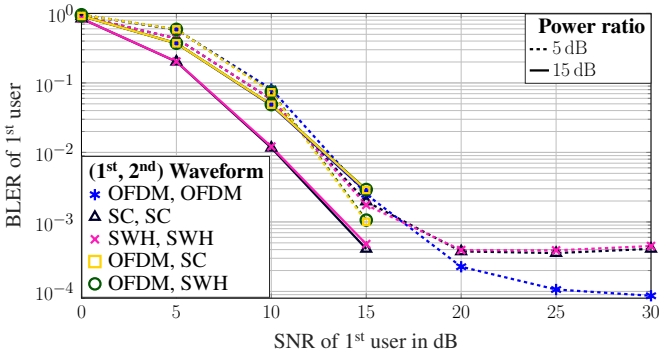

(a) BLER of 1st user

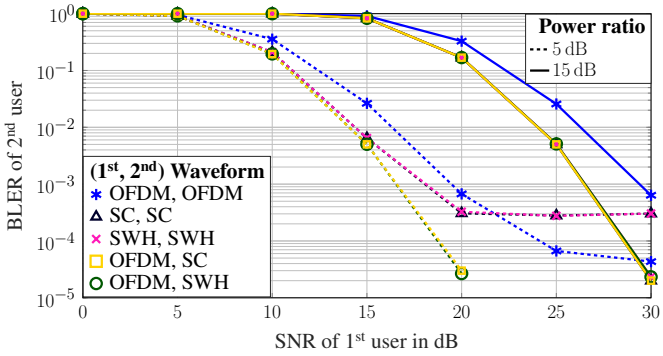

(b) BLER of 2nd user

Fig. 6: BLER for different power ratios and $N_{\text{SIC}} = 2$

At a power ratio of 5 dB, more inter-user interference (IUI) is present. For the 1st user, all the waveform combinations achieve a similar BLER until an SNR of 15 dB. At higher SNR (SWH,SWH), (SC,SC) and (OFDM,OFDM) have noise floor which is lower for the latter. For the 2nd user, a similar noise floor occurs for the same waveforms. However, for (OFDM,SC) and (OFDM,SWH) no noise floor appears for the observed range of the BLER. This is due to the fact that the OFDM waveform for the 1st user generates good a-priori estimates for IC (cf. IV-A) and the frequency spreading lead to a low BLER for the weak 2nd user.

In summary, the mixed waveforms perform better than using the same waveform for both users. Additionally, the combination (OFDM,SWH) can be considered as the best low-complexity solution among the studied combinations, due to the sparsity of the SWH modulation matrix.

V. Conclusion

In this paper, a general framework and an iterative receiver are derived for power-domain NOMA to enable the combination and analysis of different waveforms. The designed receiver integrates soft-information SIC with an MMSE-PIC detector. To investigate the potential of mixed waveform for NOMA, three waveforms, namely OFDM, SC, SWH, have been evaluated in different combinations considering two users in a frequency selective channel. It has been numerically shown that the system with mixed waveforms performs better than using the same waveform for both users, especially at low power ratios. In particular, when OFDM is utilized for the user with the higher power and SC or SWH for the other user. With this configuration, a higher fairness is achieved for both users with regard to the BLER. Moreover, the combination of OFDM and SWH arises as a potential practical mixed waveform candidate due to its low-complexity implementation.

To determine whether the advantages of using mixed waveforms for two users can be extended to more users, the analysis of $K > 2$ users is subject to our future research work.

Acknowledgment

This project has received funding from the European Union's Horizon 2020 research and innovation programme through the project iNGENIOUS under grant agreement No. 957216.

References

[1] L. Dai, B. Wang, Z. Ding, Z. Wang, S. Chen, and L. Hanzo, "A Survey of Non-Orthogonal Multiple Access for 5G," *IEEE Communications Surveys Tutorials*, vol. 20, no. 3, pp. 2294–2323, 2018.

[2] S. M. R. Islam, N. Avazov, O. A. Dobre, and K. Kwak, "Power-Domain Non-Orthogonal Multiple Access (NOMA) in 5G Systems: Potentials and Challenges," *IEEE Communications Surveys Tutorials*, vol. 19, no. 2, pp. 721–742, 2017.

[3] M. B. Shahab, S. J. Johnson, M. Shirvanimoghaddam, M. Chafii, E. Basar, and M. Dohler, "Index Modulation Aided Uplink NOMA for Massive Machine Type Communications," *IEEE Wireless Communications Letters*, vol. 9, no. 12, pp. 2159–2162, 2020.

[4] M. M. Şahin and H. Arslan, "Waveform-Domain NOMA: The Future of Multiple Access," in *2020 IEEE International Conference on Communications Workshops (ICC Workshops)*, 2020, pp. 1–6.

[5] M. B. Çelebi and H. Arslan, "Theoretical Analysis of the Co-Existence of LTE-A Signals and Design of an ML-SIC Receiver," *IEEE Transactions on Wireless Communications*, vol. 14, no. 8, pp. 4626–4639, 2015.

[6] A. Maatouk, E. Çalışkan, M. Koca, M. Assaad, G. Gui, and H. Sari, "Frequency-Domain NOMA With Two Sets of Orthogonal Signal Waveforms," *IEEE Communications Letters*, vol. 22, no. 5, pp. 906–909, 2018.

[7] Z. Ding, R. Schober, P. Fan, and H. Vincent Poor, "OTFS-NOMA: An Efficient Approach for Exploiting Heterogenous User Mobility Profiles," *IEEE Transactions on Communications*, vol. 67, no. 11, pp. 7950–7965, 2019.

[8] M. Matthé, D. Zhang, and G. Fettweis, "Low-Complexity Iterative MMSE-PIC Detection for MIMO-GFDM," *IEEE Transactions on Communications*, vol. 66, no. 4, pp. 1467–1480, 2018.

[9] R. Bomfin, M. Chafii, and G. Fettweis, "Low-Complexity Iterative Receiver for Orthogonal Chirp Division Multiplexing," in *2019 IEEE Wireless Communications and Networking Conference Workshop (WCNCW)*, 2019, pp. 1–6.

[10] A. Molisch, *Wireless Communications*. Wiley-IEEE Press, 2011.

[11] R. Bomfin, D. Zhang, M. Matthé, and G. Fettweis, "A Theoretical Framework for Optimizing Multicarrier Systems Under Time and/or Frequency-Selective Channels," *IEEE Communications Letters*, vol. 22, no. 11, pp. 2394–2397, 2018.

[12] R. Bomfin, A. Nimr, M. Chafii, and G. Fettweis, "A Robust and Low-Complexity Walsh-Hadamard Modulation for Doubly-Dispersive Channels," *IEEE Communications Letters*, pp. 1–1, 2020.

[13] C. Studer, S. Fateh, and D. Seethaler, "ASIC Implementation of Soft-Input Soft-Output MIMO Detection Using MMSE Parallel Interference Cancellation," *IEEE Journal of Solid-State Circuits*, vol. 46, no. 7, pp. 1754–1765, 2011.

[14] A. Winkelbauer, N. Goertz, and G. Matz, "Compress-and-forward in the multiple-access relay channel: With or without network coding?" 08 2012, pp. 131–135.

[15] 3GPP, "LTE; Evolved Universal Terrestrial Radio Access (E-UTRA); Base Station (BS) conformance testing," 3rd Generation Partnership Project (3GPP), Technical Specification (TS) 36.141, 10 2010, v8.4.0.